

Exhaled CO₂ as a COVID-19 Infection Risk Proxy for Different Indoor Environments and Activities

Zhe Peng and Jose L. Jimenez*



Cite This: *Environ. Sci. Technol. Lett.* 2021, 8, 392–397



Read Online

ACCESS |



Metrics & More

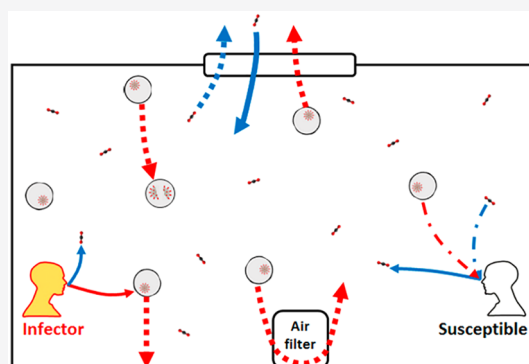


Article Recommendations



Supporting Information

ABSTRACT: CO₂ is co-exhaled with aerosols containing SARS-CoV-2 by COVID-19-infected people and can be used as a proxy of SARS-CoV-2 concentrations indoors. Indoor CO₂ measurements by low-cost sensors hold promise for mass monitoring of indoor aerosol transmission risk for COVID-19 and other respiratory diseases. We derive analytical expressions of CO₂-based risk proxies and apply them to various typical indoor environments. The relative infection risk in a given environment scales with excess CO₂ level, and thus, keeping CO₂ as low as feasible in a space allows optimization of the protection provided by ventilation. We show that the CO₂ level corresponding to a given absolute infection risk varies by >2 orders of magnitude for different environments and activities. Although large uncertainties, mainly from virus exhalation rates, are still associated with infection risk estimates, our study provides more specific and practical recommendations for low-cost CO₂-based indoor infection risk monitoring.



INTRODUCTION

Coronavirus disease 2019 (COVID-19) is currently sweeping the world and causing major losses of human life.¹ Lockdowns imposed to various extent worldwide for the COVID-19 transmission reduction are not supposed to be long-term measures, otherwise they lead to unaffordable social and economic costs. On the other hand, resumption of social, educational, and business activities raises concerns about transmission resurgence.

In past few months, there has been rapidly mounting evidence for COVID-19 transmission via aerosols,^{2–5} i.e., severe acute respiratory syndrome coronavirus 2 (SARS-CoV-2)-containing particles with diameters of <100 μm that can float in the air for minutes to hours. Such aerosols have been detected in exhaled air of COVID-19 patients⁶ and in hospital air,^{7,8} and the behaviors of smaller ones out of the proximity of sources have been shown to be similar to those of gas.^{9,10} Transmission is much easier indoors than outdoors, which is most consistent with aerosols.^{4,11,12} As humans spend most of their time in indoor environments, where air volumes are limited and virus-laden aerosols may easily accumulate, mitigation of indoor COVID-19 transmissions is a subject of great interest^{13,14} and is key to a successful societal and economic reopening. Practical, affordable, and widely applicable measures for monitoring and limiting indoor transmission risks are urgently needed.

Direct measurements of virus-containing aerosols are extremely difficult and slow. Indoor CO₂ was suggested as an indicator of ventilation of indoor spaces in the 19th century,¹⁵ and more recently as a practical proxy of respiratory infectious

disease transmission risk,¹⁶ as pathogen-containing aerosols and CO₂ are co-exhaled by those infected (Figure 1). Because the background (ambient) CO₂ level is almost stable and indoor excess CO₂ is usually only from human exhalation, measurements of indoor CO₂ concentrations by low-cost CO₂ sensors can often be good indicators of infection risk and suitable for mass deployment.^{17,18} However, the CO₂ level corresponding to a given COVID-19 infection risk is largely unknown. A few guideline limit concentrations have been proposed, but without a solid and quantitative basis.^{19,20} In particular, only a single CO₂ threshold was recommended in each of these proposed guidelines. Whether a single CO₂ concentration ensures a low COVID-19 infection risk in all common indoor environments remains an open question but is also critical for effective CO₂-based mass risk monitoring.

In this study, we derive the analytical expressions of the probability of indoor COVID-19 infection through room-level aerosol transmission only (i.e., assuming social distance is kept so that close proximity aerosol and droplet pathways are eliminated; fomite transmission is not included), human-exhaled CO₂ concentration, and subsequently a few CO₂-based quantities as infection risk proxies. On the basis of available

Received: March 8, 2021

Revised: April 1, 2021

Accepted: April 2, 2021

Published: April 5, 2021



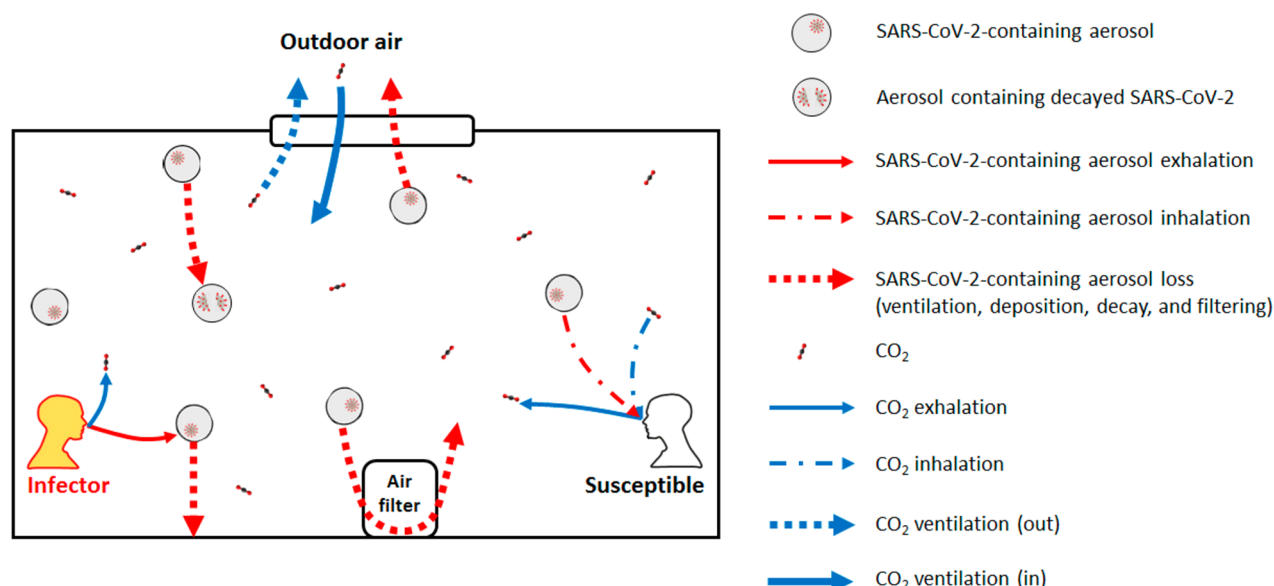


Figure 1. Schematic illustrating the exhalation, inhalation, and other loss processes of SARS-CoV-2-containing aerosols and the exhalation, inhalation, and other sources and sinks of CO₂ in an indoor environment.

data, we apply these expressions to common indoor settings to answer the open question mentioned above.

MATERIALS AND METHODS

To derive the SARS-CoV-2 aerosol concentration in indoor air, we assume well-mixed air (Figure 1). The degree of inhomogeneity can be easily quantified with portable low-cost sensors. If significant inhomogeneity in indoor air is present, the indoor space can often be approximated as several compartments, each of them having relatively well-mixed air. Ventilation with outdoor air, decay of virus and deposition of virus onto surfaces, and additional control measures [e.g., air filtration and use of germicidal ultraviolet (UV) radiation] result in losses of infective virus from indoor air. Other sinks (e.g., inhalation by humans and animals indoors) are assumed to be insignificant. This model will underestimate the risk in environments with significant nonrespiratory sources of infective aerosols (e.g., bathrooms due to toilet flushing, resuspension in healthcare facilities due to donning and doffing of personal protective equipment). The amount of the virus infectious doses (n , “quanta”) inhaled by a susceptible person determines their probability of infection (P) (see Table S1 for the list of symbols in this study). According to the Wells–Riley model of aerosol infection²¹

$$P = 1 - e^{-n} \quad (1)$$

One SARS-CoV-2 quantum corresponds to a probability of infection of $1 - 1/e$ (63%). The expected value of n ($\langle n \rangle$) for an originally uninfected person corresponding to a given level of immunity in the local population (probability of an occupant being immune, η_{im}) can be calculated as follows

$$\langle n \rangle = (1 - \eta_{\text{im}})c_{\text{avg}}BD(1 - m_{\text{in}}) \quad (2)$$

where c_{avg} , B , D , and m_{in} are the average virus concentration (quanta per cubic meter), the breathing rate of the susceptible person (cubic meters per hour), the duration of the event (hours), and the mask filtration efficiency for inhalation, respectively. The term $1 - \eta_{\text{im}}$ is included because quanta inhaled by an immune uninfected individual will not lead to

infection and should be excluded. Under the assumption of no occupants and no SARS-CoV-2 in the indoor air at the start of the event, the analytical expression of the expected value of c_{avg} based on the prevalence of infectors in the local population (probability of an occupant being an infector, η_{i}), $\langle c_{\text{avg}} \rangle$, is (see Section S1 of the Supporting Information for the derivation)

$$\langle c_{\text{avg}} \rangle = \frac{\eta_{\text{i}}(N - 1)E_{\text{p}}(1 - m_{\text{ex}})}{V} \left(\frac{1}{\lambda} - \frac{1 - e^{-\lambda D}}{\lambda^2 D} \right) \quad (3)$$

where N is number of occupants, E_{p} is the SARS-CoV-2 exhalation rate by an infector (quanta per hour), m_{ex} is the mask filtration efficiency for exhalation, V is the indoor environment volume (cubic meters), and λ is the first-order overall rate constant of the virus infectivity loss (inverse hours) that includes the ventilation with outdoor air and all other virus removal and deactivation processes.

If there are no other significant CO₂ sources or sinks (e.g., gas/coal stove and pets/plants), i.e., if indoor excess CO₂ (relative to the background outdoor level) production is only due to human exhalation and its loss is ventilation, similar quantities for CO₂ can be expressed as follows (see Section S1 for the derivation)

$$n_{\Delta\text{CO}_2} = \Delta c_{\text{avg,CO}_2}BD \quad (4)$$

$$\Delta c_{\text{avg,CO}_2} = \frac{NE_{\text{p,CO}_2}}{V} \left(\frac{1}{\lambda_0} - \frac{1 - e^{-\lambda_0 D}}{\lambda_0^2 D} \right) \quad (5)$$

where $n_{\Delta\text{CO}_2}$, $\Delta c_{\text{avg,CO}_2}$, and $E_{\text{p,CO}_2}$ are the inhaled excess (human-exhaled) CO₂ volume (cubic meters), the excess CO₂ volume mixing ratio, and the CO₂ exhalation rate per person (cubic meters per hour), respectively, and λ_0 is the ventilation rate (inverse hours).

When P is low, as it should be for a safe reopening, $P \approx n$. As airborne SARS-CoV-2 and excess CO₂ are co-exhaled and co-inhaled, in principle $n_{\Delta\text{CO}_2}$ can be a proxy of $\langle n \rangle$, and thus P . The ratio of $n_{\Delta\text{CO}_2}$ to $\langle n \rangle$ (in cubic meters per quantum)

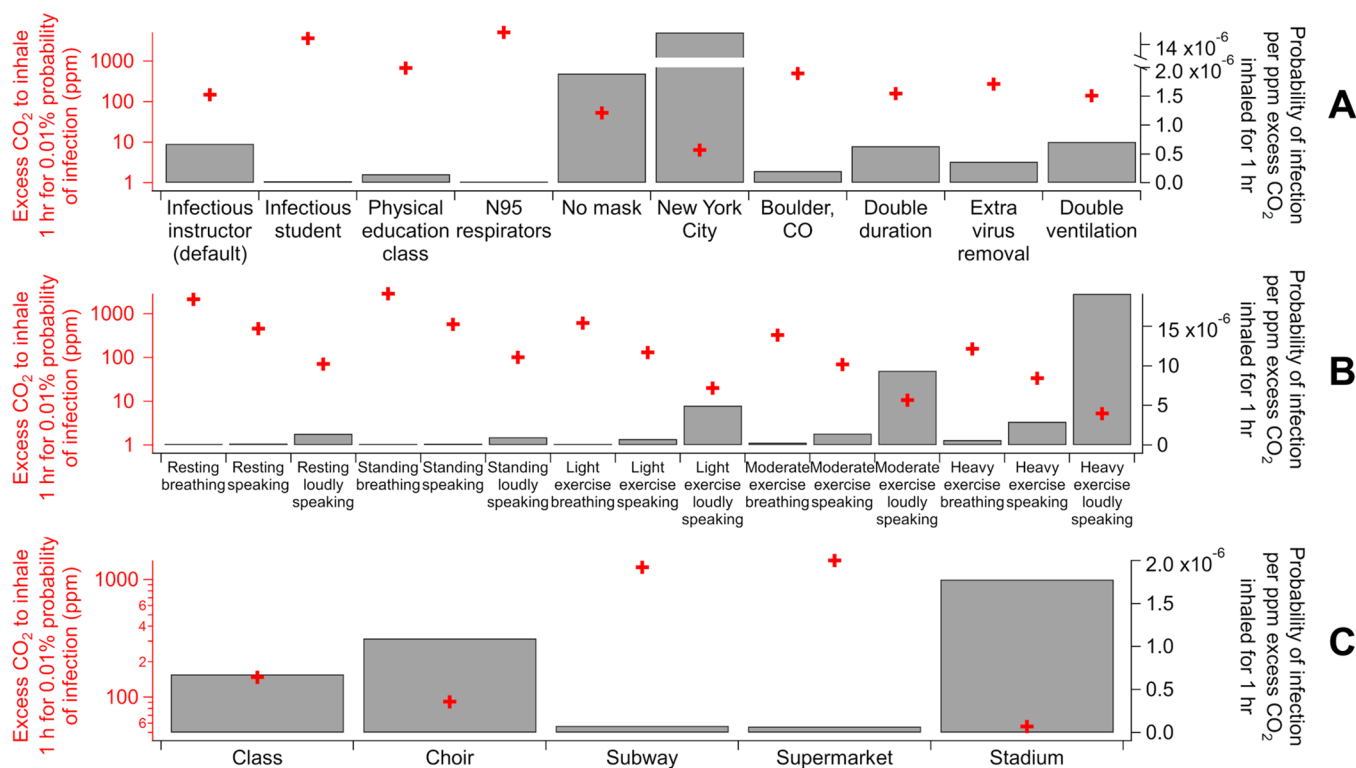


Figure 2. Excess CO_2 volume mixing ratio (parts per million) that an uninfected individual inhales for 1 h for a probability of infection of 0.01% ($\Delta c_{\text{CO}_2}^*$) and probability of infection per parts per million excess CO_2 inhaled for 1 h (inversely proportional to $\Delta c_{\text{CO}_2}^*$) with a probability of an occupant being an infector of 0.1% (except the New York City and Boulder, CO, cases in panel A and the choir case in panel C) for (A) variants of the university class case (see Table S2 for the case details), (B) various activities (see Table S3 for details of the activities), and (C) several indoor environments (see Table S4 for the case details).

$$\frac{n_{\Delta\text{CO}_2}}{\langle n \rangle} = \frac{NE_{p,\text{CO}_2}}{(1 - \eta_{\text{im}})\eta_{\text{I}}(N - 1)E_p(1 - m_{\text{ex}})(1 - m_{\text{in}})} \times \frac{\frac{1}{\lambda_0} - \frac{1 - e^{-\lambda_0 D}}{\lambda_0^2 D}}{\frac{1}{\lambda} - \frac{1 - e^{-\lambda D}}{\lambda^2 D}} \quad (6)$$

indicates the volume of inhaled excess CO_2 corresponding to a unit inhaled quantum. However, this quantity, involving inhaled CO_2 volume that is difficult to measure, is not practical for widespread transmission risk monitoring, which usually requires a fast decision-making process simply based on the indoor CO_2 concentration reading (usually in parts per million) of a low-cost sensor. Therefore, we propose, as another proxy of the risk of an environment with $\eta_{\text{I}} = 0.1\%$, the reference excess CO_2 level ($\Delta c_{\text{CO}_2}^*$), i.e., the volume mixing ratio of excess CO_2 that an uninfected individual inhales for a typical duration (1 h) in that environment for a typical probability of infection (0.01%).

$$\Delta c_{\text{CO}_2}^* = \frac{0.0001/1\text{h} \times NE_{p,\text{CO}_2}}{(1 - \eta_{\text{im}})\eta_{\text{I}}(N - 1)E_p(1 - m_{\text{ex}})(1 - m_{\text{in}})B} \times \frac{\frac{1}{\lambda_0} - \frac{1 - e^{-\lambda_0 D}}{\lambda_0^2 D}}{\frac{1}{\lambda} - \frac{1 - e^{-\lambda D}}{\lambda^2 D}} \quad (7)$$

This quantity is closely related to the excess CO_2 level corresponding to the unity basic reproduction number (R_0)¹⁶ (see Section S2) and can be directly and easily compared to

CO_2 sensor readings. The ratio of the excess CO_2 reading to $\Delta c_{\text{CO}_2}^*$ is that of the probability of infection of an originally uninfected person in that environment for 1 h to 0.01%. $\Delta c_{\text{CO}_2}^*$ scales (roughly) linearly with most of the parameters in eq 7 (see discussions below). A P of 0.01% being chosen as the reference does not imply safety at this P in all situations, because when N and/or D is large, and/or the event is repeated many times (e.g., in school/university settings), the overall probability of infection for one susceptible person and/or total infections may still be significant.

RESULTS AND DISCUSSION

The reference excess CO_2 level is a function of a number of variables. A priori, varying any of them can result in a different value of $\Delta c_{\text{CO}_2}^*$ even for similar settings. As an example, we study a set of model cases for a typical university class. The cases are specified in Table S2. The $\Delta c_{\text{CO}_2}^*$ and $\frac{n_{\Delta\text{CO}_2}}{n}$ in these cases are shown in Figure 2A and Figure S1A, respectively.

In the base class case, the infector is assumed to be the instructor. Compared to the case with a student being the infector, $\Delta c_{\text{CO}_2}^*$ in the base case is ~ 1.5 orders of magnitude lower, just because the vocalization of the instructor, who usually speaks, greatly enhances E_p ,^{22,23} while virus exhalation by students, who are assumed here to speak little, is much less efficient. In the case of a physical education (PE) class in the same indoor environment, where occupants are assumed to be doing heavy exercise and no talking, $\Delta c_{\text{CO}_2}^*$ is much lower than

for the infected student case in a traditional lecture (Figure 2A). Compared to sitting, heavy exercise increases both occupants' virus and CO₂ exhalation rates to similar extents,^{22–24} which does not significantly change the reference excess CO₂ level. However, breathing rates of occupants doing intense activities are much higher than those sitting.²⁵ Even if CO₂ and SARS-CoV-2 concentrations are the same as in the infected student case, a susceptible person in the PE class case can still inhale a larger dose of SARS-CoV-2 and more excess CO₂ and have a remarkably different *P*. As a result, a single recommendation of indoor CO₂ threshold is not valid even for a series of school settings. The range of CO₂ levels measured in real-world classrooms is very large.²⁶ The reference excess CO₂ level of the infectious student case (relatively safe) is exceeded in some classrooms, while that of the infectious instructor case (relatively risky) is met in other classrooms.

According to eqs 2 and 3, whether occupants wear masks and what masks they wear can make a substantial difference in infection risk through virus filtration in the same indoor setting. However, masks do not filter CO₂. The base class case (with surgical masks), that with all occupants wearing N95 respirators, and that with no mask use have identical CO₂ mixing ratios, but an up to ~2 order of magnitude different probability of infection (Table S2) due to filtration of virus-containing particles by mask. Therefore, for the same probability of infection of 0.01%, the base class case is estimated by eq 7 to have a corresponding excess CO₂ level 30 times lower than the case with all occupants wearing N95 respirators but ~2 times higher than the case with no mask use (Figure 2A).

η_1 is obviously another important factor governing the infection risk, as *P* is proportional to it. Again, it has no impact on CO₂. Compared to the base class case ($\eta_1 = 0.001$), the estimated situations of similar classes in New York City (NYC) in April ($\eta_1 = 0.023$) and in Boulder, CO, in June ($\eta_1 = 0.0003$) have ~20 times higher and ~2 times lower values of *P*, respectively (Table S2), and hence $\Delta c_{\text{CO}_2}^*$ values proportionally lower and higher, respectively (Figure 2A). Note that $\Delta c_{\text{CO}_2}^*$ is smaller than the current typical accuracy of low-cost CO₂ sensors (± 50 ppm)²⁷ and cannot be meaningfully measured by those sensors in very risky situations such as the NYC case here. Closure of environments with such low permissible $\Delta c_{\text{CO}_2}^*$ is likely needed. However, η_{im} usually cannot result in a difference in *P* greater than a factor of 2 under conditions of interest, because if $\eta_{\text{im}} > 50\%$, the population has reached or is close to herd immunity²⁸ and widespread transmission risk monitoring is no longer needed.

According to eq 7, the other variables that can affect $\Delta c_{\text{CO}_2}^*$ are *N*, *D*, λ , and λ_0 . $\Delta c_{\text{CO}_2}^*$ is generally not highly sensitive to them, although some of them (e.g., λ) can have a large impact on *P*. As long as occupants are not only a few, $\frac{N}{(N-1)}$, where *N* plays a role in eq 7, is close to 1. The fraction term including *D*, λ , and λ_0 (after the product sign) in eq 7 usually does not deviate from 1 substantially (Figure S2). It is close to 1 when λD is very small and λ/λ_0 when λD is very large. As long as the indoor environment is not very poorly ventilated or equipped with very strong virus removal setups (e.g., substantial filtering of recirculated air, portable HEPA filters, and germicidal UV), λ/λ_0 is relatively close to 1. Compared to the base classroom case ($\lambda/\lambda_0 \sim 1.3$), doubling the duration or ventilation causes

minimal changes in $\Delta c_{\text{CO}_2}^*$. Increasing λ/λ_0 to ~3 by additional virus control measures increases $\Delta c_{\text{CO}_2}^*$ more significantly, as those measures do not remove CO₂, but this change is still within a factor of 2 for the range of control measures in these examples (Figure 2A).

As discussed above, occupants' activities indoors, to which *E_p*, *E_{p,CO2}*, and *B* are all related, are a major or dominant factor governing the infection risk. We thus compile the data of these parameters as a function of activity (intensity and vocalization degree) (Table S3). Note that this compilation has large uncertainties from *E_p* data^{22,23} and matching of activity categories, which are all classified differently for *E_p*, *E_{p,CO2}*, and *B* (see Section S3 for details). These uncertainties are currently difficult to quantify but likely large enough to be the dominant uncertainty sources for the model output. Other sources of uncertainty are thus not discussed. Further systematic uncertainty analyses would be of interest. However, the trends shown are clear and thus able to reveal the relative risk of these activities with confidence. Simply, the stronger the vocalization, the higher the risk, and the more intense activity, the higher the risk. We calculate $\Delta c_{\text{CO}_2}^*$ for these activities when *N* is large, *D* = 1 h, $\eta_1 = 0.001$, $\lambda_0 = 3 \text{ h}^{-1}$, $\lambda = 4 \text{ h}^{-1}$, and no mask is used (Figure 2B), a setting similar to the class case. Three class cases, i.e., base, infected student, and PE cases, can be easily related to the activity categories of “standing–loudly speaking”, “resting–breathing”, and “heavy exercise–breathing”, respectively. The related pairs have $\Delta c_{\text{CO}_2}^*$ values within a factor of ~2, and their mask use setting and close but different *E_p*, *E_{p,CO2}*, and *B* values can largely explain the differences in $\Delta c_{\text{CO}_2}^*$.

Then we apply this analysis to a range of real-world settings, in addition to the class case, i.e., the Skagit County choir superspreading event,⁵ a subway car, a supermarket (focused on a worker), and an event in a stadium, which, though outdoors, often has somewhat stagnant air allowing virus-laden aerosols to build up and thus can be treated like an indoor environment (see Table S4 for the specifications of these cases). Figure 2C and Figure S1B show their $\Delta c_{\text{CO}_2}^*$ and $\frac{n_{\text{ACO}_2}}{n}$, respectively. Again, these values span orders of magnitude. We can still relate these cases to the activity categories of “standing–loudly speaking”, “resting–breathing”, “light exercise–breathing” (or “light exercise–speaking”), and “light exercise–speaking” (or “light exercise–loudly speaking”).

For the actual choir case, its η_1 is an order of magnitude lower than 0.1% while the estimated *E_p* is an order of magnitude higher (20), resulting in a reference excess CO₂ level similar to that of “standing–loudly speaking” shown in Figure 2B. $\Delta c_{\text{CO}_2}^*$ in the stadium case is between those of “light exercise–speaking” and “light exercise–loudly speaking”, as both activities may happen during the event. The difference in $\Delta c_{\text{CO}_2}^*$ between the supermarket case and its related activities shown in Figure 2B is mainly due to the long duration of the event (8 h). The $\Delta c_{\text{CO}_2}^*$ of the supermarket case divided by the duration leads to the excess CO₂ threshold for the worker to inhale over 8 h between those of “light exercise–breathing” and “light exercise–speaking”. The $\Delta c_{\text{CO}_2}^*$ of the subway case is ~1/3 lower than that of “resting–breathing” in Figure 2B

because of the short duration (0.33 h) and mask use (universal use of surgical masks or equivalent).

As shown above, the infection risk analysis for various settings can be based on the relevant activities with adjustments for η , D , mask use, etc. For policy making concerning an acceptable indoor CO_2 level, we also recommend an activity-dependent approach. Reference excess CO_2 levels for indoor environments with certain types of activities mainly involved can be found in Figure 2B. Then, this mixing ratio can be scaled for typical D (by multiplying it) and target P (by multiplying its ratio to 0.01%) to obtain an excess CO_2 threshold, which may be relaxed a little further depending on the local mask policy. The sum of this value and the local outdoor CO_2 concentration, the latter of which we recommend measuring regularly due to possible variations,²⁹ is the final recommended indoor CO_2 concentration threshold. For more complex setups (e.g., with many CO_2 meters in a company or school), a meter should be located outdoors to measure CO_2 concentration continuously. To the best of our knowledge, CO_2 is the only quantity that can be easily measured by fast low-cost sensors as an infection risk proxy. The relative risk of infection in a given situation has been shown to scale with the excess CO_2 concentration. The absolute risk can be estimated when the parameters needed are known. Calculations for various scenarios can be easily performed with the online COVID-19 aerosol transmission estimator.³⁰ Then this method can provide a stronger scientific basis for using CO_2 than having one threshold for all situations. However, it may still not be trivial for the general public to estimate the parameters used in our model and implement it. Regulatory authorities may derive the CO_2 thresholds for different types of indoor spaces or provide more assistance for businesses to do so. Even if the parameters are unknown, our study suggests that simply keeping the CO_2 level and the physical intensity and vocalization level of the activities as low as practically feasible in indoor environments will still reduce the risk.

■ ASSOCIATED CONTENT

Supporting Information

The Supporting Information is available free of charge at <https://pubs.acs.org/doi/10.1021/acs.estlett.1c00183>.

Discussions about the relationship between the reference excess CO_2 level and the Rudnick–Milton model, details of the mathematical derivations and of how the values of major parameters are assigned, a list of the cases of interest, values of the large fraction term in eqs 6 and 7, and a table of the symbols used in this study (PDF)

■ AUTHOR INFORMATION

Corresponding Author

Jose L. Jimenez – Cooperative Institute for Research in Environmental Sciences and Department of Chemistry, University of Colorado, Boulder, Colorado 80309, United States; orcid.org/0000-0001-6203-1847; Email: jose.jimenez@colorado.edu

Author

Zhe Peng – Cooperative Institute for Research in Environmental Sciences and Department of Chemistry, University of Colorado, Boulder, Colorado 80309, United States; orcid.org/0000-0002-6823-452X

Complete contact information is available at:

<https://pubs.acs.org/doi/10.1021/acs.estlett.1c00183>

Notes

The authors declare no competing financial interest.

This paper has been previously submitted to medRxiv, a preprint server for health sciences. The preprint can be cited as Peng, Z.; Jimenez, J. L. Exhaled CO_2 as COVID-19 infection risk proxy for different indoor environments and activities. 2021. *medRxiv* 10.1101/2020.09.09.20191676 (accessed 2021-04-01).

■ ACKNOWLEDGMENTS

The authors thank Demetrios Pagonis and Bertrand Waucquez for useful discussions.

■ REFERENCES

- (1) World Health Organization. *Coronavirus Disease (COVID-2019) Situation Reports*; 2021.
- (2) Prather, K. A.; Marr, L. C.; Schooley, R. T.; McDiarmid, M. A.; Wilson, M. E.; Milton, D. K. Airborne Transmission of SARS-CoV-2. *Science* **2020**, *370* (6514), 303.2–304.
- (3) Tang, J. W.; Bahnfleth, W. P.; Bluyssen, P. M.; Buonanno, G.; Jimenez, J. L.; Kurnitski, J.; Li, Y.; Miller, S.; Sekhar, C.; Morawska, L.; et al. Dismantling Myths on the Airborne Transmission of Severe Acute Respiratory Syndrome Coronavirus-2 (SARS-CoV-2). *J. Hosp. Infect.* **2021**, *110*, 89–96.
- (4) Morawska, L.; Milton, D. K. It Is Time to Address Airborne Transmission of Coronavirus Disease 2019 (COVID-19). *Clin. Infect. Dis.* **2020**, *71* (9), 2311–2313.
- (5) Miller, S. L.; Nazaroff, W. W.; Jimenez, J. L.; Boerstra, A.; Buonanno, G.; Dancer, S. J.; Kurnitski, J.; Marr, L. C.; Morawska, L.; Noakes, C. Transmission of SARS-CoV-2 by Inhalation of Respiratory Aerosol in the Skagit Valley Chorale Superspreading Event. *Indoor Air* **2021**, *31* (2), 314–323.
- (6) Ma, J.; Qi, X.; Chen, H.; Li, X.; Zhang, Z.; Wang, H.; Sun, L.; Zhang, L.; Guo, J.; Morawska, L.; et al. Coronavirus Disease 2019 Patients in Earlier Stages Exhaled Millions of Severe Acute Respiratory Syndrome Coronavirus 2 Per Hour. *Clin. Infect. Dis.* **2020**, DOI: [10.1093/cid/ciaa1283](https://doi.org/10.1093/cid/ciaa1283).
- (7) Liu, Y.; Ning, Z.; Chen, Y.; Guo, M.; Liu, Y.; Gali, N. K.; Sun, L.; Duan, Y.; Cai, J.; Westerdahl, D.; et al. Aerodynamic Analysis of SARS-CoV-2 in Two Wuhan Hospitals. *Nature* **2020**, *582* (7813), 557–560.
- (8) Lednicky, J. A.; Lauzardo, M.; Fan, Z. H.; Jutla, A.; Tilly, T. B.; Gangwar, M.; Usmani, M.; Shankar, S. N.; Mohamed, K.; Eiguren-Fernandez, A.; et al. Viable SARS-CoV-2 in the Air of a Hospital Room with COVID-19 Patients. *Int. J. Infect. Dis.* **2020**, *100*, 476–482.
- (9) Bond, T. C.; Bosco-Lauth, A.; Farmer, D. K.; Francisco, P. W.; Pierce, J. R.; Fedak, K. M.; Ham, J. M.; Jathar, S. H.; VandeWoude, S. Quantifying Proximity, Confinement, and Interventions in Disease Outbreaks: A Decision Support Framework for Air-Transported Pathogens. *Environ. Sci. Technol.* **2021**, *55* (5), 2890–2898.
- (10) Ai, Z.; Mak, C. M.; Gao, N.; Niu, J. Tracer Gas Is a Suitable Surrogate of Exhaled Droplet Nuclei for Studying Airborne Transmission in the Built Environment. *Build. Simul.* **2020**, *13* (3), 489–496.
- (11) Chen, W.; Zhang, N.; Wei, J.; Yen, H.-L.; Li, Y. Short-Range Airborne Route Dominates Exposure of Respiratory Infection during Close Contact. *Build. Environ.* **2020**, *176*, 106859.
- (12) Tellier, R.; Li, Y.; Cowling, B. J.; Tang, J. W. Recognition of Aerosol Transmission of Infectious Agents: A Commentary. *BMC Infect. Dis.* **2019**, *19* (1), 101.
- (13) Qian, H.; Miao, T.; Liu, L.; Zheng, X.; Luo, D.; Li, Y. Indoor Transmission of SARS-CoV-2. *Indoor Air* **2020**, DOI: [10.1111/ina.12766](https://doi.org/10.1111/ina.12766).

- (14) Morawska, L.; Tang, J. W.; Bahnfleth, W.; Bluyssen, P. M.; Boerstra, A.; Buonanno, G.; Cao, J.; Dancer, S.; Floto, A.; Franchimon, F.; et al. How Can Airborne Transmission of COVID-19 Indoors Be Minimised? *Environ. Int.* **2020**, *142*, 105832.
- (15) de Chaumont, F. On the Theory of Ventilation: An Attempt to Establish a Positive Basis for the Calculation of the Amount of Fresh Air Required for an Inhabited Air-Space. *Proc. R. Soc. London* **1875**, *23*, 187–201.
- (16) Rudnick, S. N.; Milton, D. K. Risk of Indoor Airborne Infection Transmission Estimated from Carbon Dioxide Concentration. *Indoor Air* **2003**, *13* (3), 237–245.
- (17) Martin, C. R.; Zeng, N.; Karion, A.; Dickerson, R. R.; Ren, X.; Turpie, B. N.; Weber, K. J. Evaluation and Environmental Correction of Ambient CO₂ Measurements from a Low-Cost NDIR Sensor. *Atmos. Meas. Tech.* **2017**, *10* (7), 2383–2395.
- (18) Mendell, M. J.; Eliseeva, E. A.; Davies, M. M.; Spears, M.; Lobscheid, A.; Fisk, W. J.; Apte, M. G. Association of Classroom Ventilation with Reduced Illness Absence: A Prospective Study in California Elementary Schools. *Indoor Air* **2013**, *23* (6), 515–528.
- (19) Jones, E.; Young, A.; Clevenger, K.; Salimifard, P.; Wu, E.; Luna, M. L.; Lahvis, M.; Lang, J.; Bliss, M.; Azimi, P.; et al. *Healthy Schools: Risk Reduction Strategies for Reopening Schools*; 2020.
- (20) Cheng, S.-Y.; Wang, C. J.; Shen, A. C.-T.; Chang, S.-C. How to Safely Reopen Colleges and Universities During COVID-19: Experiences From Taiwan. *Ann. Intern. Med.* **2020**, *173*, 638–641.
- (21) Riley, E. C.; Murphy, G.; Riley, R. L. Airborne Spread of Measles in a Suburban Elementary School. *Am. J. Epidemiol.* **1978**, *107* (5), 421–432.
- (22) Buonanno, G.; Stabile, L.; Morawska, L. Estimation of Airborne Viral Emission: Quanta Emission Rate of SARS-CoV-2 for Infection Risk Assessment. *Environ. Int.* **2020**, *141* (April), 105794.
- (23) Buonanno, G.; Morawska, L.; Stabile, L. Quantitative Assessment of the Risk of Airborne Transmission of SARS-CoV-2 Infection: Prospective and Retrospective Applications. *Environ. Int.* **2020**, *145*, 106112.
- (24) Persily, A.; de Jonge, L. Carbon Dioxide Generation Rates for Building Occupants. *Indoor Air* **2017**, *27* (5), 868–879.
- (25) Chapter 6—Inhalation Rates. In *Exposure Factors Handbook*; U.S. Environmental Protection Agency, 2011.
- (26) Fromme, H.; Heitmann, D.; Dietrich, S.; Schierl, R.; Körner, W.; Kiranoglu, M.; Zapf, A.; Twardella, D. Raumluftqualität in Schulen - Belastung von Klassenräumen Mit Kohlendioxid (CO₂), Flüchtigen Organischen Verbindungen (VOC), Aldehyden, Endotoxinen Und Katzenallergenen. *Das Gesundheitswes* **2008**, *70* (2), 88–97.
- (27) Aranet. Wireless Indoor Air Monitoring, CO₂, Temperature, Humidity Sensor. <https://aranet.com/product/aranet4-sensor/> (accessed 2021-02-26).
- (28) Britton, T.; Ball, F.; Trapman, P. A Mathematical Model Reveals the Influence of Population Heterogeneity on Herd Immunity to SARS-CoV-2. *Science* **2020**, *369* (6505), 846–849.
- (29) Dias Carrilho, J.; Mateus, M.; Batterman, S.; Gameiro da Silva, M. Air Exchange Rates from Atmospheric CO₂ Daily Cycle. *Energy Build.* **2015**, *92*, 188–194.
- (30) Jimenez, J. L.; Peng, Z. COVID-19 Aerosol Transmission Estimator (<https://tinyurl.com/covid-estimator>).